GLAS-PPE/2005-07

Department of Physics & Astronomy
Experimental Particle Physics Group
Kelvin Building, University of Glasgow
Glasgow, G12 8QQ, Scotland
Telephone: ++44 (0)141 339 8855 Fax: +44 (0)141 330 5881

A comparison between irradiated Magnetic Czochralski and Float Zone silicon detectors using the Transient Current Technique

Alison G Bates[a,b] and Michael Moll[b]

[a] Department of Physics and Astronomy
University of Glasgow, Scotland
Email: a.bates@physics.gla.ac.uk
[b] *CERN, PH-Department, CH-1211, Geneva 23, Switzerland*

Abstract

Magnetic Czochralski (MCz) silicon has recently become a promising material for the development of radiation tolerant detectors for future high luminosity HEP experiments. A thorough study of 24 GeV/c proton irradiated p^+- in - n FZ, DOFZ and MCz silicon detectors has been conducted using the standard radiation damage characterization tools IV and CV, the Transient Current Technique (TCT) and annealing studies. The first systematic study on the effective trapping time in MCz silicon has been performed. The results show that the introduction rate for the traps responsible for the degradation of the effective trapping time for MCz material agrees with the introduction rate for FZ and DOFZ silicon. From the behaviour of the depletion voltage as a function of proton fluence and through the TCT technique, it has been shown that by a radiation fluence of 5×10^{14} p/cm^2 the depletion voltage has passed its minimum value without type inversion. An annealing study compares the evolution of the effective trapping time, the effective space charge density and the current related damage parameters for MCz and DOFZ silicon.

1. Introduction

Silicon detectors will be used in all of the 5 experiments due to start taking data at the LHC accelerator in 2007. These very high luminosity experiments with design luminosities up to $10^{34}cm^{-2}s^{-1}$ and even more the proposed future upgrade of the LHC towards a luminosity of $10^{35}cm^{-2}s^{-1}$ [1, 2] demand the development of detectors which can be used to cover large surface areas and perform in extremely harsh radiation levels. The radiation damage suffered by the silicon results in an increase of leakage current, a change of full depletion voltage and an increased trapping of the drifting holes and electrons created by traversing charged particles. These three effects reduce the Charge Collection Efficiency, CCE, and the signal to noise ratio of the detector.

Almost all detectors currently used in HEP use silicon grown by the Float Zone (FZ) technique. The FZ growth method yields high purity and high resistivity silicon, suitable for high energy particle physics tracking and detection. The ROSE collaboration [3] proved that diffusing oxygen into the bulk silicon of a detector increases the detector's radiation hardness towards charge particle irradiation [4]. The oxygen concentration of FZ silicon detectors is in the order of a few 10^{16} cm^{-3}. However, this concentration can be increased to some 10^{17} cm^{-3} through an oxygen diffusion processing step. Silicon which has undergone this additional oxygenation process is called Diffusion Oxygenated Float Zone (DOFZ) silicon.

Recent technological advances have led to the development of high resistivity magnetic Czochralski (MCz) silicon which now can be produced with a resistivity of up to a few kΩcm [5]. With this technique it is possible to control the oxygen concentration through the melt flow rate and the rate of evaporation of oxygen from the surface of the melt [5]. MCz has typically an oxygen concentration of 2-5 x $10^{17}cm^{-3}$ which is intrinsic due to the growth process. With such a high oxygen concentration, it is expected to offer increased radiation tolerance when compared to FZ and DOFZ silicon. There exist only a few studies comparing the radiation tolerance of MCz silicon detectors to the one of DOFZ or FZ silicon detectors [6- 10]. All the previous studies have found MCz silicon to be more radiation tolerant and the majority of studies have found indications that MCz silicon does not type invert, however, so far no clear proof could be given that there is no type inversion in MCz silicon.

This paper presents a thorough study of the radiation tolerance of MCz in comparison to DOFZ and FZ silicon using CV, IV and the Transient Charge Technique (TCT). Although TCT has been extensively used before to characterize FZ and DOFZ silicon detectors, this paper will present the first systematic TCT study on MCz silicon detectors.

In the next section TCT, which has been used to characterize the effective trapping times in DOFZ, FZ and MCz silicon, is described. Section 3 will outline the material used in this study and provide details about the irradiation procedure. Finally, section 4 presents the results obtained with the above mentioned techniques on FZ, DOFZ and MCz silicon detectors. All results are compared to previously published data, where data is available.

2. Transient Current Technique (TCT)

Irradiation of silicon detectors results in the creation of defects in the silicon lattice which potentially can trap the charge carriers produced by traversing particles. If the integration time of the electronics is less than the time to de-trap the charge then the measured signal is reduced. For the LHC experiments the integration time is strongly constrained as the time between bunch crossings will be only 25 ns. The Transient Current Technique (TCT) allows us to understand how much charge can be collected as a function of the integration time and gives accurate information on the effective trapping time of charge carriers drifting through the silicon detector. The method used in this work to extract the effective trapping time is called the "Charge Correction Method" [11,12] and will be briefly described below. TCT can also be used to determine the depletion voltage of a device through a Charge-Voltage (QV) measurement and, by analyzing the shape of the TCT signal, the sign of the effective space charge can be determined.

TCT is based on the detection of one dominant type of charge carrier, electron or hole, which drifts across the entire detector thickness, for illustration, one assumes the detector is of type p^+-n-n^+. This can be achieved by illuminating the front (p^+) implant or rear (n^+) implant of the detector with a pulsed laser diode having a wavelength in the red region. The red light penetrates the silicon only by a few microns creating equal numbers of electrons and holes. One type of the charge carriers (electrons or holes) will immediately be absorbed by the nearest implant while the other type of charge carrier will have to drift across the entire detector thickness (typically 300 μm). This will lead to the domination of the signal by one type of carrier. The current resulting from the type of carrier which travels only a short distance is induced in a very short time and the signal is usually damped strongly by the rise-time of the electronic system. The current for the carriers traversing the whole detector thickness is induced over a longer period and will thus dominate the observed signal. A hole dominated signal (hole injection) can be achieved by illuminating the rear n^+ implant of the detector. In this case the electrons will be immediately collected at the n^+ implant.

The effective trapping probability, $1/\tau_{eff}$, is the probability that a carrier is lost due to trapping in the silicon. $Q_{e,h}(t)$ is the charge obtained from integration of the current, I(t). Fig. 1 shows the relationship between Q(t) and I(t) for an electron injection signal (dashed lines).

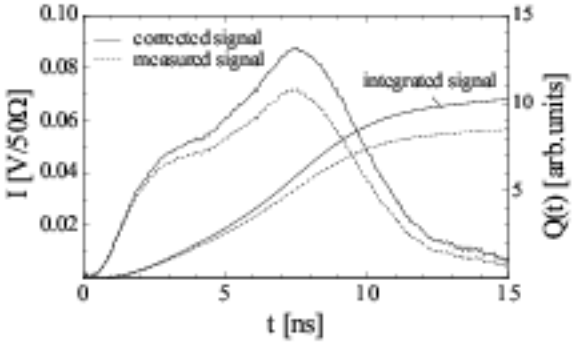

Fig. 1.: Example of an electron injection signal collected before (dashed) and after (solid line) the correction for the trapped charge. FZ test detector (15kΩcm, irradiated to 5.2×10^{13} 24GeV/c p/cm^2, V_{fd} = 30 V) measured at 90 V. CCM method resulted in $\tau_{eff,e}$ = 37.8 ns. The integrated charge, Q(t), is also shown (right hand axis). Please note, t_o has been set to zero.

When the detector has been irradiated the drifting charge, $Q_{e,h}(t)$, will be lost with an exponential time dependence due to trapping in the defects,

$$Q_{e,h}(t) = Q_{e,h}(t_o)\exp\left(\frac{-(t-t_o)}{\tau_{eff_{e,h}}}\right) . \qquad (1)$$

$Q_{e,h}(t_o)$ is the initial charge created at the point of the charge injection. τ_{eff} is the effective trapping time defined through the definition of the trapping probability;

$$\frac{1}{\tau_{eff_{e,h}}} = \sum_x N_x\left(1 - P_x^{e,h}\right)\sigma_{x_{e,h}} v_{th_{e,h}} . \qquad (2)$$

N_x is the concentration of the individual 'x' trap which captures the charge carrier, $P_x^{e,h}$ is the probability of the trap occupation with either carrier and $\sigma_{x\ e,h}$ is the carrier capture cross section. $v_{th\ e,h}$ is the thermal velocity of the carrier. The probability is summed over all defect types, x, which may lead to charge carrier trapping.

The measured induced charge, $Q_{e,h}(t)$, can be corrected for the charge lost due to trapping

$$Q_{e,h}(t_o) = Q_{e,h}(t)\exp\left(\frac{t-t_o}{\tau_{eff_{e,h}}}\right) , \qquad (3)$$

where t_0 is the time of the carrier injection. If the measured induced charge has been corrected for the trapped charge, the integrated charge should be the same for all voltages above the full depletion voltage. The gradient of the integrated corrected charge as a function of voltage above the full depletion voltage should be zero if the value of τ_{eff} is correct. If the value of τ_{eff} is varied, the gradient of the corrected charge as a function of voltage will vary. The true value of τ_{eff} is found when the gradient is zero. This is the Charge Correction Method (CCM) which was independently proposed in [11] and [12]. Fig. 1 shows an example of an electron injection signal

before and after the charge correction. The CCM assumes three conditions:

- There exists one dominant trapping time
- The detrapping effects are negligible in the readout time
- All the lost charge is due to trapping

The method requires no knowledge of the electric field profile in the detector or any information about the charge carrier distributions.

All plots presented in this paper have been deconvoluted from the electronic transfer function of the TCT readout circuit and corrected for the trapped charge.

3. Experimental setup and materials

3.1. TCT, CV and IV measurements

All TCT measurements presented in this paper have been performed at (5.0±0.1)ºC, except for the study on the temperature dependence in section 4.4. The 660 nm laser diode was pulsed at a frequency of 170 Hz and the laser output had a rise time of 1.5 ns and a FWHM of between 1.6-2.0 ns. The TCT DAQ was controlled by a computer with a standard GPIB bus. Charge-Voltage (QV) measurements were performed by integrating the current pulse for various different bias voltages.

Current-Voltage (IV) and Capacitance-Voltage (CV) measurements were performed using a Keithley 2410 as a source meter, an Agilent 4263B LCR meter operating at 10 kHz in parallel mode and a Keithley 237 as a current meter. The DC supply voltage was decoupled from the small AC voltage of the LCR meter using capacitors. The rear n^+ ohmic contact was connected to the bias voltage, the guard ring was connected to the ground and the signal line was connected to the front p^+ aluminium contact. The measurements were made at room temperature T. The leakage current measured, I(T), was corrected to T_{ref} = 20ºC using equation 4.

$$I(T_{ref}) = \left(\frac{T_{ref}}{T}\right)^2 \exp\left(\frac{-E_g}{2k_B}\left[\frac{1}{T_{ref}} - \frac{1}{T}\right]\right) I(T) \quad (4)$$

E_g is the silicon band gap (1.12eV) and k_B is Boltzmann constant.

The depletion voltage V_{fd} was found from the CV method by fitting straight lines to the *log*C versus *log*V plot and determining the intercept. Similarly the depletion voltage was found from fitting straight lines to the linear and constant sections of the *log*I versus *log*V plots for the IV method and from fitting straight lines to the linear and constant sections of the Q versus V plots for the QV method.

3.2. Silicon Diodes

Table 1 gives the details about the four investigated types of silicon material. All devices consisted of n-type bulk material with p^+-implants for the pad of the detector. The pad area was approximately 5 x 5 mm^2. The thickness of the devices has been carefully measured and varies between 295-304 µm with a 2% measurement error. However, the implant thickness of the detectors processed at the Helsinki Institute of physics is 3.5 µm hence twice this value is subtracted to get the active thickness for each device [13]. Each detector

Table 1. H.I.P is the Helsinki Institute of Physics, Finland and ST is ST Microelectronics, Italy. The initial depletion voltage was measured from the intercept of the two straight lines fitted to the *log-log* capacitance-voltage graphs.

Sample name	Silicon type	Manufacturer	Crystal orientation	ρ [kΩcm]	Processing	Oxygenation	Thickness [µm]	Initial V_{fd} [V]
f2	FZ	Okmetric Oyj	<1 00>	1	H.I.P	-	295 ± 2	235 ± 15
d1	DOFZ	Okmetric Oyj	<1 00>	1	H.I.P	75h at 1100ºC	295 ± 2	269 ± 7
W317	DOFZ	Wacker	<1 1 1>	15	ST	60 h at 1200ºC	300 ± 2	14 ± 2
n320	MCz	Okmetric Oyj	<1 00>	1	H.I.P	-	304 ± 2	309 ± 5

has either a single or multiple guard ring structure. The guard rings were connected for the CV and IV measurements but were left floating for all of the TCT measurements. An opening of approximately 2 mm in diameter was left in the top metallization to enable the laser light to penetrate the silicon lattice and for the same reason the n^+ back side had a grid structure of metal.

Two types of DOFZ detectors (d1 and W317) were studied in order to compare the detectors processed at the Helsinki Institute of Physics to detectors which have been processed at ST Microelectronics. Studies have also been conducted to compare the FZ, DOFZ and MCz silicon processed at the Helsinki Institute of Physics.

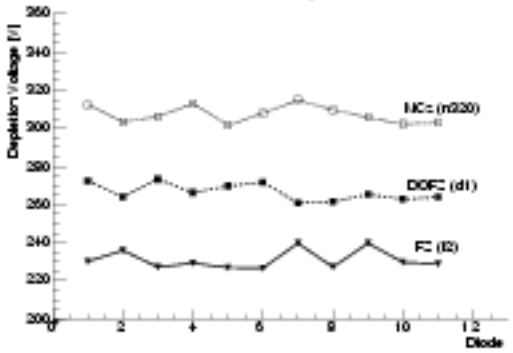

Fig. 2. Depletion voltage extracted from the CV method for 11 tested MCz, DOFZ and FZ silicon detectors before irradiation.

3.3. Irradiations

All diodes were irradiated at 27ºC using 24 GeV/c p at the CERN PS [14]. The range of fluences achieved was (1.7–60) x 10^{13} p/cm^2. The fluence received was measured through spectroscopy of aluminum foil placed with the detectors in the PS beam during irradiation [14]. A hardness factor of 0.62 was used to convert the 24 GeV/c proton fluence into 1 MeV equivalent neutron fluence [15].

For each fluence two detectors of each material type were irradiated to improve statistics. After the irradiations the detectors were annealed for 4 minutes at 80ºC. At all other times the detectors were stored at -23ºC to minimise further annealing.

4. Characterization

4.1. Leakage Current

The temperature corrected leakage currents, at the full depletion voltage, were normalised to the active volume of the detector and are shown in Fig. 3 as a function of the fluence in 1MeV neutron non-ionizing energy loss (NIEL) equivalent. The behaviour is linear with a proportionality constant α called the current related damage rate:

$$\alpha = \frac{I}{vol \times \Phi_{eq}} \qquad (5)$$

The active volume of the detector is *vol* and Φ_{eq} is the 1 MeV neutron equivalent fluence which previously has been measured to be material independent [16] and have a value of α(4min/80ºC) = 4.56 x 10^{-17} A/cm [17]. Table 2 shows the values of α obtained for the four detector materials under study. No significant difference between the materials is observed and the obtained α-values are in good agreement with previously published data (see Table 2).

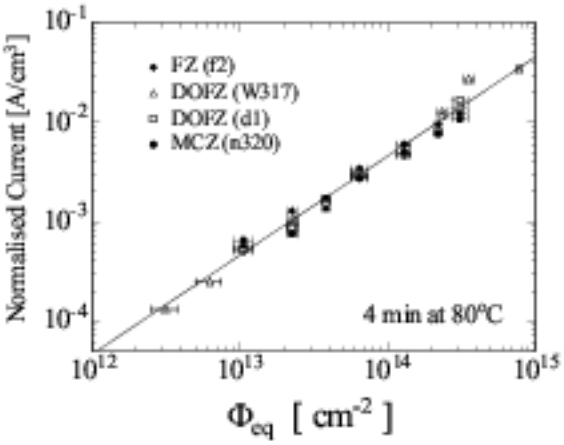

Fig. 3.: Leakage current scaled to 20ºC and normalized to the detector volume as a function of 1 MeV neutron equivalent fluence. The solid line represents the value of α = 4.56 x 10^{-17} A/cm [15].

Sample name	Silicon type	α [A/cm]
f2	FZ	4.96×10^{-17}
d1	DOFZ	4.85×10^{-17}
W317	DOFZ	4.75×10^{-17}
n320	MCz	4.73×10^{-17}
Ref. [15]	FZ	4.56×10^{-17}

Table 2. Data for α values obtained from the data presented in Fig. 3 and values found in the literature. All values were obtained after irradiation with 24 GeV/c protons and a successive annealing of 4 minutes at 80°C.

4.2. Effective Doping Concentration

The space charge of unirradiated p^+-n-n^+ detectors is positive. With increased radiation damage the effective doping concentration, N_{eff}, is reduced due to "donor removal" and acceptor generation. Above a certain fluence the bulk silicon passes through the *"type inversion"* and the space charge becomes increasingly more negative. This is a

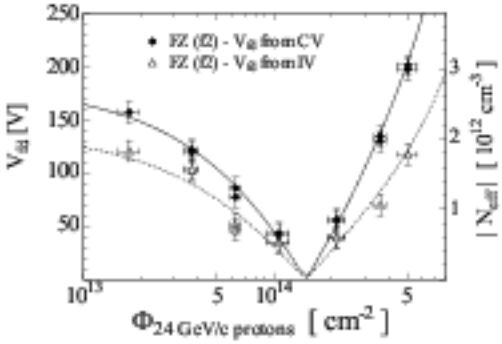

Fig. 4a. Depletion voltage of FZ silicon (f2) as function of proton fluence. Values obtained from CV (closed squares) and IV (open triangles) measurements are presented.

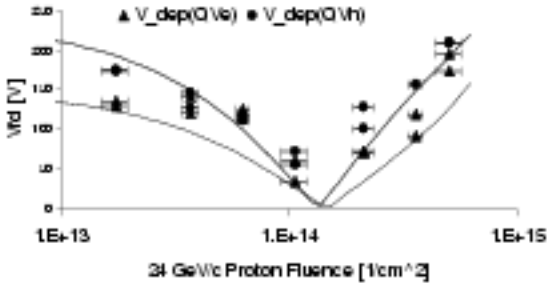

Fig. 4b. The depletion voltage, V_{fd}, of FZ silicon (f2) as a function of 24 GeV/c p/cm^2. The depletion voltage extracted from the Charge-Voltage, *QV*, method using both electron (triangles) and hole (circles) injection.

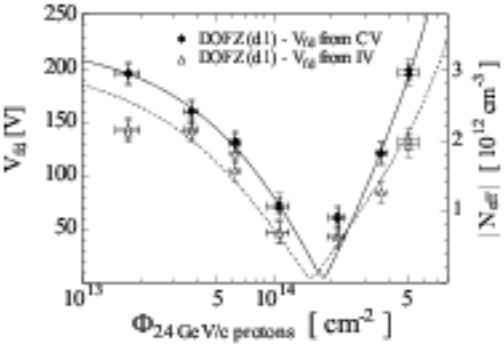

Fig. 4c. Depletion voltage of DOFZ silicon (d1) as function of proton fluence. Values obtained from CV (closed squares) and IV (open triangles) measurements are presented.

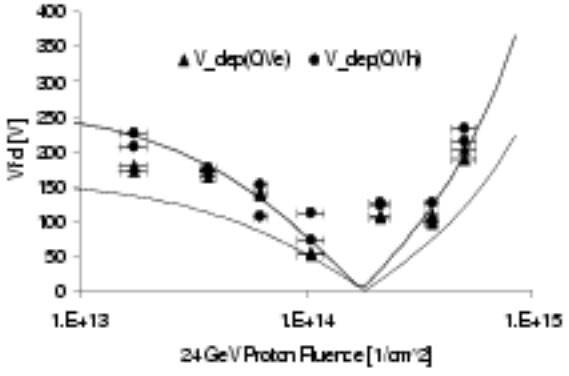

Fig. 4d. The depletion voltage, V_{fd}, of DOFZ silicon (d1) as a function of 24 GeV/c p/cm^2. The depletion voltage extracted from the Charge-Voltage, *QV*, method using both electron (triangles) and hole (circles) injection.

well known fact for FZ and DOFZ silicon detectors and is also observed in this work. The dependence of the full depletion voltage V_{fd} on the fluence is shown in Fig. 4(a-h) for the four materials studied. The effective doping concentration, which is also shown in the figures, has been calculated using

$$V_{fd} = \left| V_o \left(1 - e^{-c\Phi}\right) + g_C \Phi \right| , \qquad (7)$$

where V_o is the depletion voltage before irradiation, g_c is the net acceptor generation rate and Φ is the fluence. The fits were performed independently for

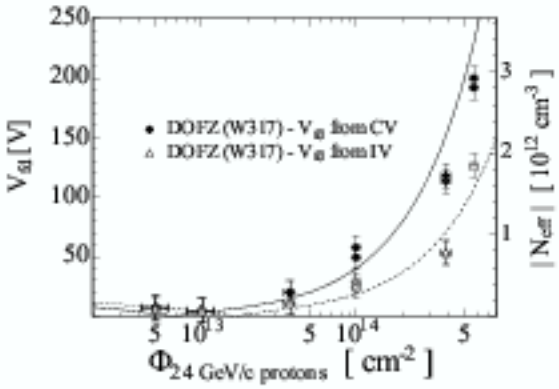

Fig. 4e. Depletion voltage of FZ silicon (W317) as function of proton fluence. Values obtained from CV (closed squares) and IV (open triangles) measurements are presented.

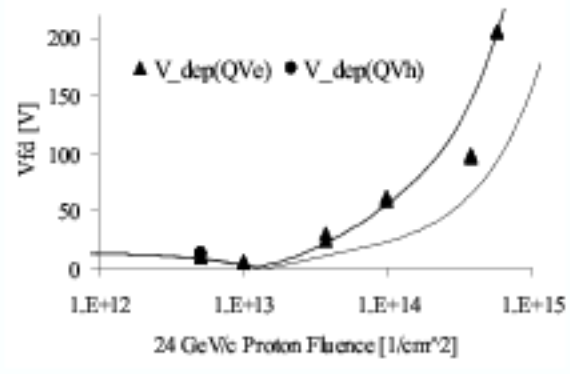

Fig. 4f. The depletion voltage, Vfd, of DOFZ silicon (W317) as a function of 24 GeV/c p/cm^2. The depletion voltage extracted from the Charge-Voltage, QV, method using both electron (triangles) and hole (circles) injection.

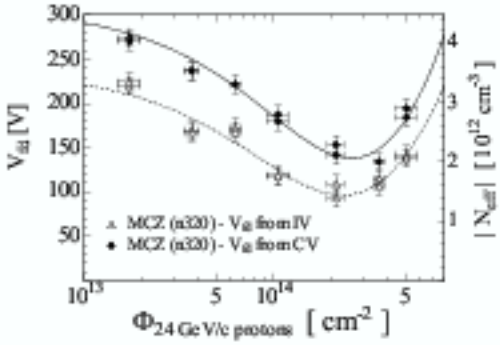

Fig. 4g. Depletion voltage of MCz silicon (n320) as function of proton fluence. Values obtained from CV (closed squares) and IV (open triangles) measurements are presented.

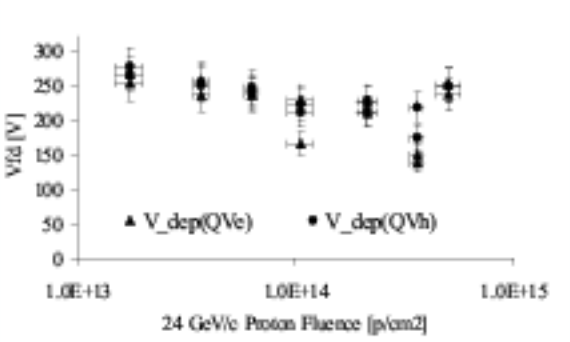

Fig. 4h. The depletion voltage extracted from the Charge-Voltage, QV, method using both electron and hole injection on MCz silicon detectors.

$$\left| N_{eff} \right| = \frac{2\,\varepsilon_{Si}\,\varepsilon_0}{q_0\,d^2}\,V_{fd} \qquad (6)$$

where $\varepsilon_{Si}\varepsilon_0$ is the permittivity of silicon, q_0 the elementary charge and d the thickness of the detector. The fit for the full depletion voltage, V_{fd}, in Fig. 4 (a-g) was calculated from equation 7,

the V_{fd} values obtained from IV, CV and QV measurements. It should be noted that in this work we did not introduce partial donor removal, since it has been shown in Ref.[4] that after 24 GeV/c proton irradiation "complete donor removal" is obtained.

	V_0 [V]		c [10^{-15}cm^2]		g_c [10^{-13}Vcm^2]	
material	IV	CV	IV	CV	IV	CV
FZ (f2)	139	182	9.22	7.48	2.43	4.14
DOFZ (d1)	207	225	9.84	6.38	2.83	4.01
DOFZ (W317)	14	14	--	--	3.05	4.00
MCz (n320)	238	309	8.65	7.15	-2.76	-3.46

Table 3. Parameters extracted from the fits described in equation 7 to the data shown in Fig. 4 (a,c,e and g).

In Fig. 4 (a-f) the depletion voltage drops to a value close to zero then increases again clearly indicating a type inversion, an assumption which will be proved by the TCT measurements presented in the next section. While the DOFZ and the FZ silicon processed at the Helsinki Institute of Physics (d1 and f2) type invert at approximately the same fluence ($\approx 1.5\times10^{14}$ p/cm^2) the low resistivity FZ type inverts at much lower fluences ($\approx 7\times10^{12}$ p/cm^2).

Contrary to the results obtained with the FZ and the DOFZ devices a less pronounced change in the depletion voltage of the MCz detectors is observed in Fig. 4g. This property is a great advantage for the application of this device material to radiation tolerant detectors.

Further clarification of the evolution of the V_{fd} of the MCz silicon was provided by extracting V_{fd} using the QV method with both hole and electron injection. The results are presented in Fig. 4h. Again, the depletion voltage is found to change only slowly with fluence. A conclusion as to whether or not the material underwent type inversion is however not possible from these measurements but will be clarified by the TCT measurements in the next section.

4.3. Space Charge Sign Inversion

Fig. 1 shows an example of electron injection into a 15 kΩcm FZ silicon detector which had been irradiated to $5.2\text{x}10^{13}$ p/cm^2. The trapping corrected current grows with increasing time over a period of 10 ns. The induced current is proportional to the drift velocity of the carriers and hence also proportional to the electric field strength. From this information alone it can be concluded that the electric field is strongest at the n^+(back) side. Hence, the silicon has undergone type inversion.

To evaluate the effective trapping time by the CCM, the applied bias voltage was always chosen to be at least 50 V above the V_{fd}, where the V_{fd} was determined by the QV method. The signal pulse was integrated over the full transient signal.

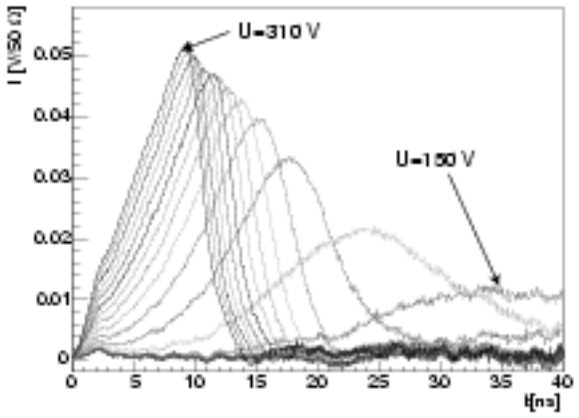

Fig. 5a. The induced current signal resulting from hole injection into a DOFZ (d1) silicon detector. The detector had been irradiated to $1.7\text{x}10^{13}$ p/cm^2 and the V_{fd} found through the hole injection-QV method was 205 V.

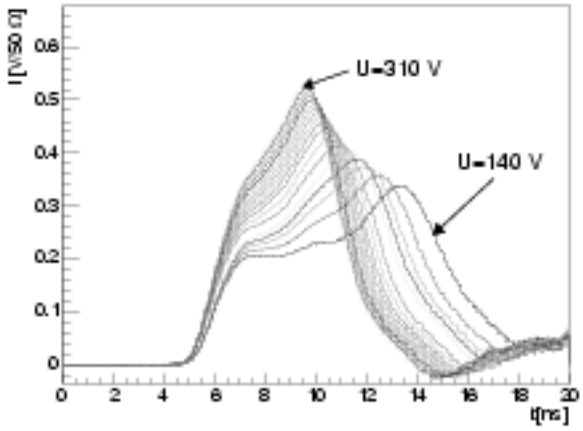

Fig. 5b. The induced current signal resulting from electron injection into a DOFZ (d1) silicon detector. The detector had been irradiated to $5.1\text{x}10^{14}$ p/cm^2 and the V_{fd} found through electron injection-QV method was 203V. Please note $t_0 = 5$ ns. The current was measured at different voltages between 140 V and 310 V, the extreme values are indicated on the plot.

Fig. 5a and Fig. 5b are the results of hole and electron injection into DOFZ (d1) silicon detectors respectively. The induced current was recorded at various bias voltages above the V_{fd} after hole injection. Fig. 5a shows an increasing current signal, hence the electric field must be growing from the front p^+ (front) implant. This shows that at a fluence of $1.7x10^{13}$ p/cm^2 the DOFZ material (d1) still has a positive space charge and is not type inverted, confirming the expectation resulting from Fig. 4c. Fig. 5b shows the current signal for electron injection into a DOFZ (d1) detector obtained after a fluence of $5.1x10^{14}$ p/cm^2. The electron induced current increases indicating that the electric field profile is growing from the rear n^+ side. This confirms that the silicon has type inverted, verifying Fig. 4c.

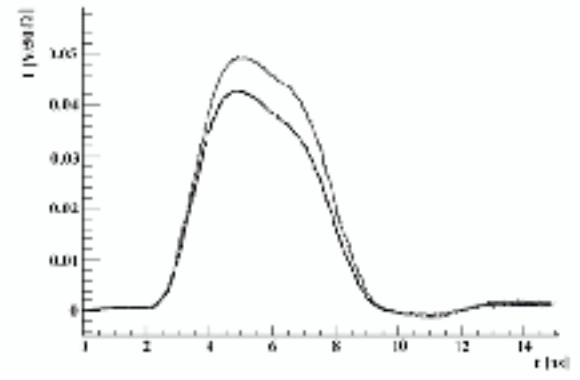

Fig. 6a. The induced current signal resulting from electron injection into a MCz silicon detector. The detector had been irradiated to $5.1x10^{14}$ p/cm^2 and the V_{fd} found through electron injection-QV method was 237V. The top dashed line is the signal after the trapping correction; the lower solid line is the electron signal before the trapping correction. The signal was measured at 370 V.

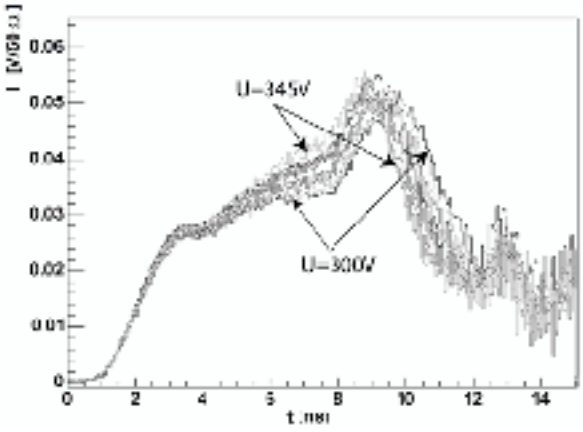

Fig. 6b. The induced current signal resulting from hole injection into a MCz silicon detector. The detector had been irradiated to $5.1x10^{14}$ p/cm^2 and the V_{fd} found through electron injection-QV method was 237V. 10 different voltages between 300 V and 345 V were tested: the extreme values are indicated on the plot.

A MCz detector was irradiated to $5.1x10^{14}$ p/cm^2 and was tested with both electron and hole injection to determine whether the silicon has type inverted, see Fig. 6a and 6b respectively. The induced signal for both measurements results in the conclusion that the MCz detector has not type inverted meaning that the bulk silicon still has a net positive space charge.

4.4. Effective trapping time

It has been shown that the effective trapping time for each carrier type, $\tau_{eff,e/h}$, for FZ silicon depends linearly on the fluence:

$$\frac{1}{\tau_{eff_{e,h}}} = \beta_{e,h}\Phi_{eq}. \qquad (8)$$

The proportionality factor, β, for both carrier types in all four materials has been measured. The linear relationship expressed in equation 8 is illustrated for both electrons and holes in Fig. 7a–7c for the FZ, DOFZ and MCz detectors. The measurements at low fluences have not been included in the straight line fits since they have a large error. The trapping time at this radiation level is expected to be in the order of

200 ns while the integration time of the signal was approximately 30 ns. Due to the relatively large difference in time scales an accurate determination of the trapping time was not possible.

Table 4 contains the β values determined for both carrier types and some values determined in previous works using a similar TCT technique.

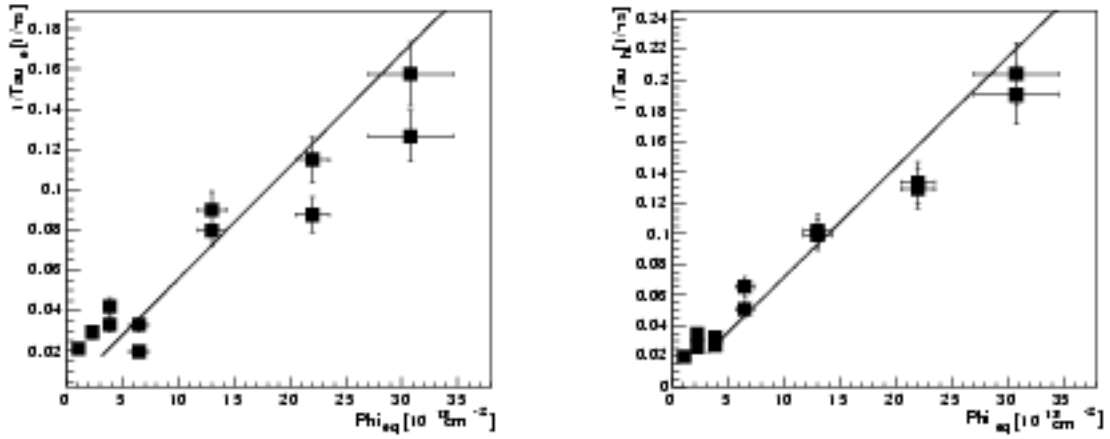

Fig. 7a. Trapping probability, $1/\tau_{eff}$, as function of fluence determined after electron (left) and hole (right) injection for FZ silicon.

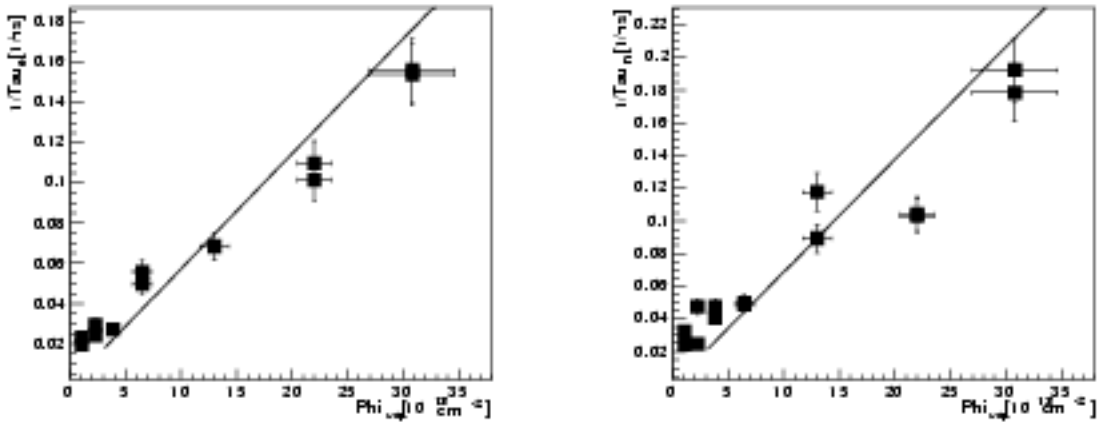

Fig. 7b. Trapping probability, $1/\tau_{eff}$, as a function of fluence determined after electron (left) and hole (right) injection for DOFZ (d1) silicon.

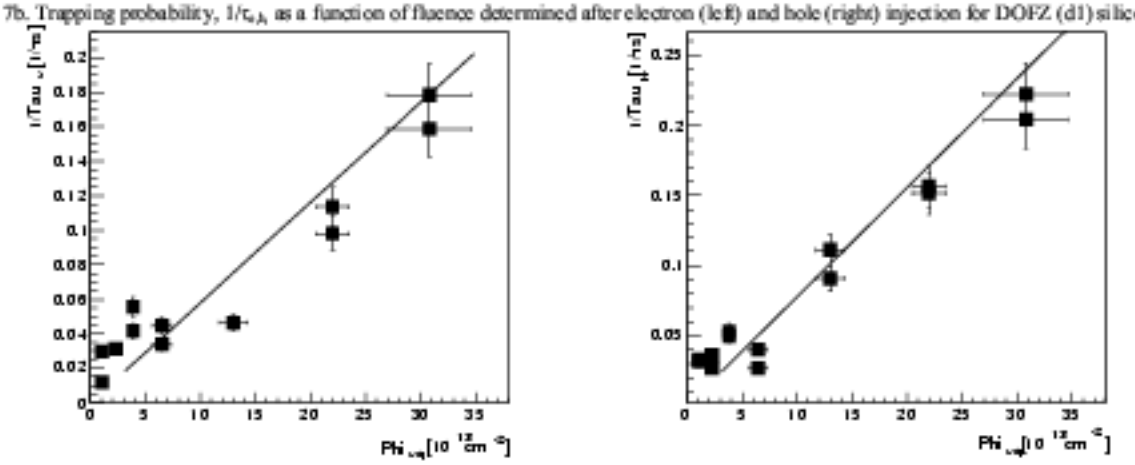

Fig. 7c. . Trapping probability, $1/\tau_{eff}$, as a function of fluence determined after electron (left) and hole (right) injection for MCz silicon.

	β_e [10^{-16} cm^2/ns]	β_h [10^{-16} cm^2/ns]
FZ (f2)	5.59 ± 0.29	7.16 ± 0.32
DOFZ (d1)	5.73 ± 0.29	6.88 ± 0.34
MCz (n320)	5.81 ± 0.32	7.78 ± 0.39
DOFZ (W317)	5.48 ± 0.22	6.02 ± 0.29
Dortmund [18] DOFZ	5.08 ± 0.16	4.90 ± 0.16
Ljubljana [19] DOFZ and FZ	5.34 ± 0.19	7.08 ± 0.18
Lancaster/Hamburg [11] FZ	5.32 ± 0.30	6.81 ± 0.29
Hamburg [20] FZ, DOFZ and MCz	5.07 ± 0.16	6.20 ± 0.54

Table 4. Comparison of β_e and β_h determined after 24 GeV/c proton irradiation. The top 4 rows are the values found in this work while the last four rows show data previously obtained by other groups. All values have been scaled to 5°C, for the temperature dependence of β (see section 4.5).

The values measured for β_e for FZ, DOFZ and MCz silicon agree within the experimental errors. The β_e values are also in approximate agreement with the previous 4 measurements by other groups. The β_h values found for the detectors under study were all about 10-30 % larger than β_e. This confirms the findings of three of the four previous studies.

Hence, this study has demonstrated that MCz and DOFZ silicon have the same trapping times as FZ silicon.

$\beta_{e,h}$ depends on the temperature of the measurement. Therefore the experimental values from the references given in Table 4 have been scaled to 5°C using a parameterization for the temperature dependence found by Kramberger [21] (see also next section). β_h has stronger temperature dependence than β_e so Hamburg's measurement made at 20°C [20], when scaled to 0°C, results in a 23% larger β_h than β_e.

4.5. Temperature Dependence

In the expression for β_e and β_h given in equation 2 there are three parameters which depend upon the temperature of the measurement, $v_{th,e,h}$ ($\propto T^{(1/2)}$), $\sigma_{e,h}$ ($\propto T^m$) and $P_x^{e,h}$, where m is an unknown constant. Assuming that there exists only one dominating trap for electrons and only one dominating trap for holes an expression can be derived for the temperature dependence (see also [21]):

$$\beta_{e,h}(T) = \beta_{e,h}(T_o)\left(\frac{1-P_t^{e,h}(T)}{1-P_t^{e,h}(T_o)}\right)\left(\frac{T}{T_o}\right)^{m+\frac{1}{2}}. \quad (10)$$

Since the constant m is poorly known and ranges between -2 and +2 [22, 23], a simplified function was fitted to the dependence of $\beta_{e,h}$ upon the temperature as proposed in [19]:

$$\beta_{e,h}(T) = \beta_{e,h}(T_o)\left(\frac{T}{T_o}\right)^{\kappa_{e,h}} \propto T^{\kappa_{e,h}}. \quad (11)$$

Where κ is a constant to be determined. Fig. 8 shows the temperature dependence of the trapping introduction rate over a 30°C range. The temperature was stable to $\pm$0.1°C. A function of the form in equation 11 was plotted for both electrons and holes. The errors on the trapping introduction rate were estimated to be about 10% arising from the error in the particle fluence (7%) and the reproducibility of the trapping time (8%) which depends on the voltage range used in the CCM analysis.

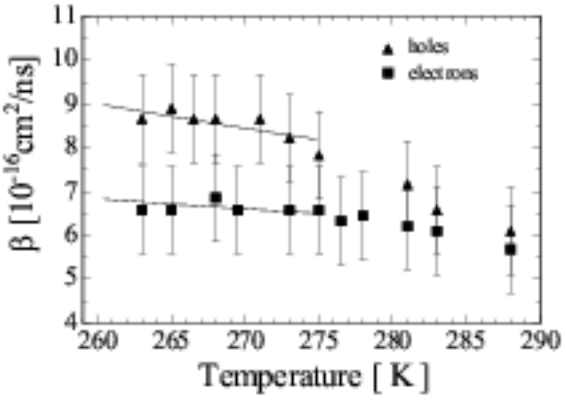

Fig. 8. Temperature dependence measured using a DOFZ (W317) silicon detector. The detector had been irradiated to 10^{14} p/cm^2.

The values extracted for $\kappa_{e,h}$ from both this study and the previous study are listed in Table 5.

Kramberger [21]	κ_e= -0.86±0.06	κ_h= -1.52±0.07
This paper	κ_e= -0.90±0.09	κ_h= -1.69±0.17

Table 5. Values for $\kappa_{e,h}$ compared to previously found values. The fit was performed in the range of 260 -275 K.

In conclusion a good agreement was found between this study and the previous study for the temperature dependence of β.

4.6. Annealing behaviour

Radiation induced defects in silicon are not stable at room temperature. Annealing effects are observed that alter the leakage current, the effective space charge density and the effective trapping times. In order to study these effects we performed isothermal annealing studies on the DOFZ and MCz silicon detectors at 80°C. Between the isothermal heating steps CV, IV and electron and hole TCT measurements were performed. The TCT signals were collected at (5.0+0.1)°C and the IV and CV measurements were done at room temperature.

4.6.1 Isothermal annealing of β_e and β_h

Fig. 9 a-c show the change of the effective trapping times as function of annealing time.

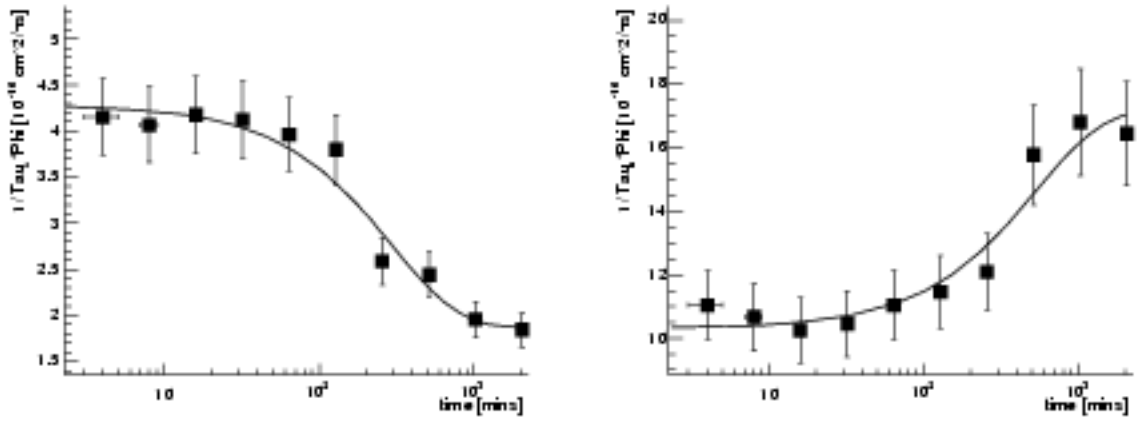

Fig. 9a. Trapping times for electrons (left) and holes (right) as a function of annealing time at 80°C for DOFZ (d1).

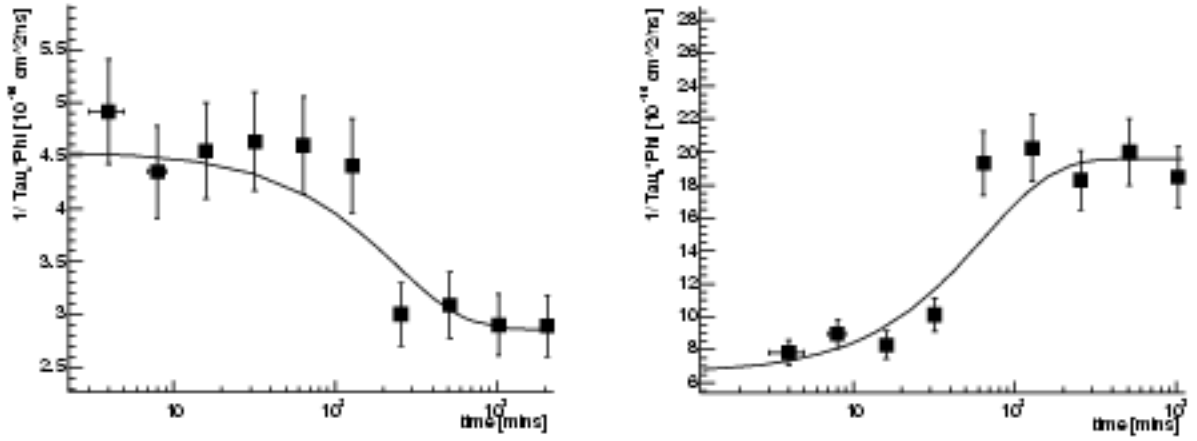

Fig. 9b. Trapping times for electrons (left) and holes (right) as a function of annealing time at 80°C for DOFZ (W317).

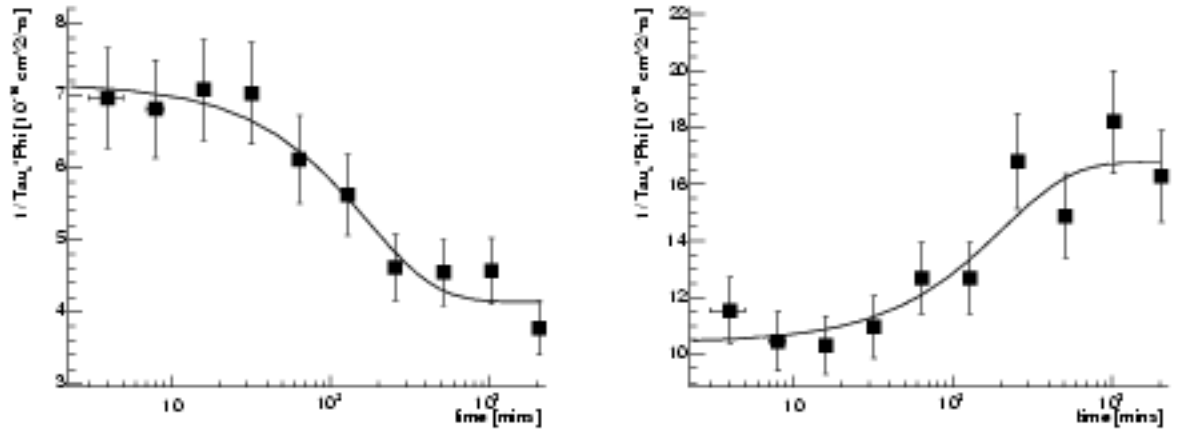

Fig. 9c. Trapping times for electrons (left) and holes (right) as a function of annealing time at 80°C for MCz.

β_e decreased by approximately 40-50%, when measured at 5°C for both types of DOFZ silicon and the MCz silicon. Moreover, β_h increases by a similar percentage. Equation 12 shows the function used to fit the measured data.

$$\beta_{e,h}(t) = \beta_{o_{e,h}} \exp\left(\frac{-t}{\tau_{e,h}}\right) + \beta_{\infty_{e,h}}\left(1 - \exp\left(\frac{-t}{\tau_{e,h}}\right)\right) \quad (12)$$

The initial and final trapping introduction rates are β_o and β_∞, respectively. Tables 6a and 6b contain the results of the fit to the annealing data.

	$\beta_{o,e}$ [10^{-16} cm^2/ns]	$\beta_{\infty,e}$ [10^{-16} cm^2/ns]	τ_e [hours]
DOFZ (d1)	4.29±0.22	1.87±0.15	4.95±1.44
DOFZ (W317)	4.54±0.24	2.86±0.20	3.92±1.70
MCz	7.16±0.42	4.14±0.26	2.86±1.32

Table 6a. The resulting fit parameters from the isothermal annealing of the electron trapping introduction rate.

	$\beta_{o,h}$ [10^{-16} cm^2/ns]	$\beta_{\infty,h}$[10^{-16} cm^2/ns]	τ_h [hours]
DOFZ (d1)	10.30±0.53	17.20±1.63	8.95±4.86
DOFZ (W317)	6.55±0.74	19.59±1.06	1.07±0.26
MCz	10.41±0.66	16.76±1.14	3.44±2.01

Table 6b. The resulting fit parameters from the isothermal annealing of the hole trapping introduction rate.

The effective trapping times were measured on the same detectors that were used as part of the study in section 4.3. All detectors had been irradiated to approximately 10^{14} p/cm^2. The errors in Table 6a and 6b come from the error in fitting. However, $\beta_{e,h}$ was determined using just one fluence point for each annealing step hence the resultant error on each fit parameter will be larger than the values quoted in Table 6a and 6b. For a more accurate determination of $\beta_{e,h}$, one should use the method described in section 4.3.

The time constants, τ_e, agree with each other within the experimental errors, however, there are some inconsistencies within the hole time constants. A previous study has shown that fit parameters on the same DOFZ W317 silicon approximately agree with this study on the initial and final trapping introduction rates [21]. Although slight differences between the values found in this study and values found in the previous studies, especially with the time constants, are apparent due to the different

temperatures used in the annealing stages. Annealing times are of the order 5 hours at 80ºC.

4.6.2 *Isothermal annealing of V_{fd} and N_{eff}*

The change of the full depletion voltage is shown in Fig. 10 and Fig. 11 as a function of annealing time at 80ºC for DOFZ silicon and MCz silicon respectively.

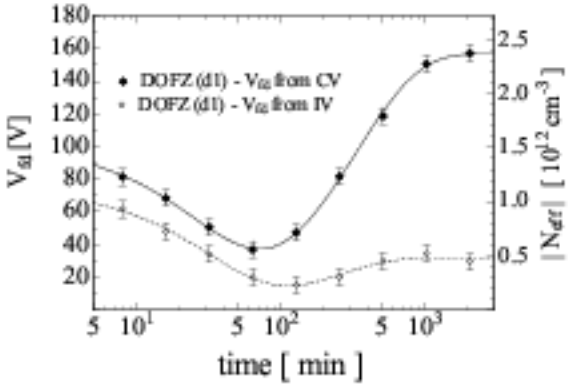

Fig. 10. The evolution of the depletion voltage as determined by CV and IV methods for DOFZ (d1) silicon. The solid line shows the fit with parameters evaluated in Table 7.

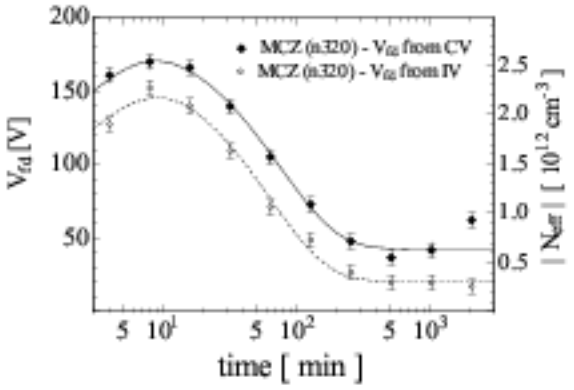

Fig. 11. The evolution of the depletion voltage as determined by CV and IV methods for MCz silicon. The solid line shows the fit with parameters evaluated in Table 7.

The depletion voltage falls then rises in Fig. 10 for DOFZ silicon irradiated to 1.1×10^{14} p/cm^2. The differences between the IV and CV methods of extracting V_{fd} highlight the large dependence of the V_{fd} value upon the method. The data presented in Fig. 10, along with the TCT signals in section 4.3, confirm that the DOFZ silicon has type inverted. Conversely, the V_{fd} of MCz is reduced with increasing annealing time, see Fig. 11. This proves that at a fluence of 10^{14} p/cm^2, MCz has not yet type inverted.

The full depletion voltage is linked to the effective doping concentration via equation 6 and the change in the effective doping concentration is defined by

$$\Delta N_{eff}\left(\Phi_{eq},t\right) = N_{eff,o} - N_{eff}\left(\Phi_{eq},t\right), \qquad (13)$$

where $N_{eff,o}$ is the effective doping concentration prior to irradiation and t is the time of isothermal annealing. There is also an annealing temperature dependence, however, throughout these studies the temperature was kept constant at 80°C and is thus not explicitly indicated in equation 13.

There have been many papers written describing the three components of the N_{eff} annealing; beneficial N_A, stable N_C and reverse N_Y (see e.g.: [17]). Equations 14-16 show the parameterization of the three components.

$$\Delta N_{eff}\left(\Phi_{eq},t\right) = N_A\left(\Phi_{eq},t\right) + N_C + N_Y\left(\Phi_{eq},t\right) \qquad (14)$$

$$N_A = g_a \Phi_{eq} \exp\left(\frac{-t}{\tau_a}\right) \qquad (15)$$

$$N_Y = N_{Y,\infty}\left(1-\exp\left(-k_{1Y}t\right)\right) \qquad (16)$$

Equation 16 is the first order parameterisation for the reverse annealing. The fit parameters are the introduction rate (g_a) and the time constant (τ_a) for beneficial annealing, the stable damage component (N_C) and the reverse annealing amplitude ($N_{Y,\infty}$) and rate constant (k_{1Y}). Fig. 12 shows the change of ΔN_{eff} as a function of isothermal annealing time for DOFZ (d1) and MCz silicon detectors.

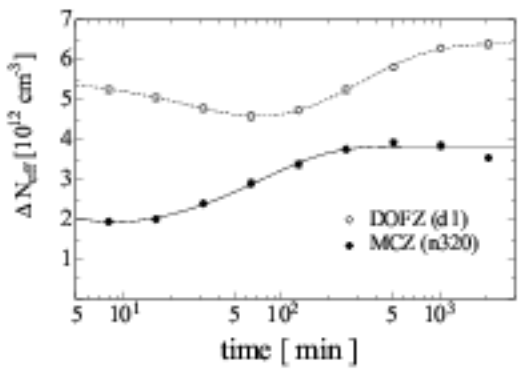

Fig. 12 .: The change of ΔN_{eff} as a function of isothermal annealing time at 80°C for DOFZ (d1) and MCz (n320)

The fits were parameterized using equations 14-16. Table 7 contains the fit parameters.

	DOFZ (d1)	MCz
χ^2/ndf	0.91/4	1.18/4
g_a [10^{-2}cm^{-1}]	2.6 ± 0.6	2.2 ± 2.6
τ_a [min]	39.0 ± 13.8	3.09 ± 2.86
N_C [10^{12}cm^{-3}]	4.08 ± 0.40	1.85 ± 0.18
$N_{Y,\infty}$ [10^{12}cm^{-3}]	2.65 ± 0.37	2.57 ± 0.17
$k_{1,Y}$ [10^{-3} min^{-1}]	2.95 ± 0.64	12.56 ± 1.79

Table 7. The results for the six parameters from the fit of the ΔN_{eff} annealing for DOFZ (d1) and MCz silicon.

The average introduction rate, g_a, for the beneficial annealing component for both DOFZ and MCz silicon is similar to the value stated in [17]:

$$g_a = (1.81 \pm 0.14) \times 10^{-2}\ \mathrm{cm}^{-1}.$$

The time constant for beneficial annealing (τ_a) had large errors from the fit and yielded very different time scales for DOFZ and MCz silicon. However, the values reflect the times associated with the minimum in Fig. 12. The reciprocal of the reverse annealing rate constant (k_{1Y}) provides a measure of the reverse time constant. The reverse time constant for DOFZ was (339 ± 74) minutes and (80 ± 11) minutes for MCz. Values previously extracted for FZ silicon were about 90 minutes [4, 17] while for DOFZ silicon a fluence dependent time constant has been found [24]. The value corresponding to the fluence used here would be 150 min which is about a factor 2 less than the value measured in this work.

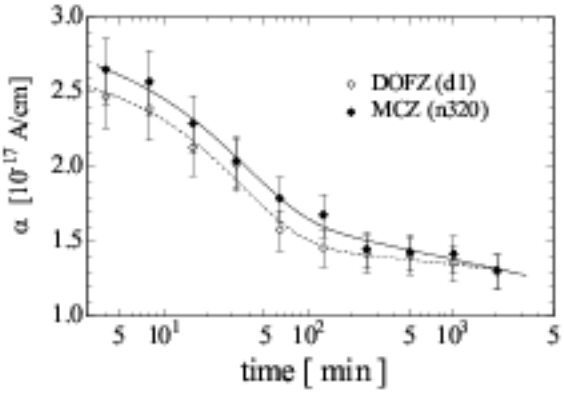

Fig. 13.: The evolution of the normalized leakage current as determined by the IV method. α is defined in equation 5.

The leakage current as a function of annealing time is presented in Fig. 13. The fit performed on the annealing of the current related damage rate, α, can be defined as described in equation 17 [16].

$$\alpha(t) = \alpha_1 \exp\left(\frac{-t}{\tau_1}\right) + \alpha_o - \beta \ell n\left(\frac{t}{\tau_0}\right) \qquad (17)$$

The parameters α_1, τ_1, α_o, τ_o and β were extracted for MCz and DOFZ silicon irradiated to approximately 10^{14} p/cm^2. τ_o was set to 1 min. No significant differences for the parameters were found between DOFZ and MCz silicon. The averaged results found for DOFZ and MCz silicon are compared to previously extracted values for annealing at 80ºC in Table 8.

	Extracted from Fig. 13	[17]
α_1 [10^{-17}A/cm]	0.9	1.13
τ_1 [min]	34	9
α_o[10^{-17}A/cm]	1.6	4.23
β [10^{-18} A/cm]	0.55	2.83

Table 8. The averaged results for the four parameters from the fit of α annealing for DOFZ (d1) and MCz silicon compared to data from Ref. [17].

5. Conclusions

A thorough study of proton irradiated p^+-in-n FZ, DOFZ and MCz silicon detectors has been conducted with the aim of developing silicon with increased radiation hardness for high luminosity HEP experiments. Through the powerful Transient Current Technique it has been shown that MCz silicon does not type invert up to a 24 GeV/c proton fluence of $5x10^{14}$ p/cm^2. The first systematic study of the effective trapping time in MCz silicon has been performed and the results show that the trap introduction rate for MCz agrees with the rate for FZ and DOFZ silicon.

An annealing study compared the evolution of the trapping, effective carrier concentration and the current related damage parameters for MCz and DOFZ silicon.

Acknowledgments

This work was performed within the framework of the RD50 collaboration. The authors thank the Helsinki Institute of Physics for supplying the silicon diodes used in the studies and Maurice Glaser and Federico Ravotti for the irradiations performed in the CERN PS. We also wish to thank Gregor Kramberger for supplying the TCT analysis software and Katharina Kaska, from the University of Technology in Vienna, who assisted with some of the measurements presented in this paper.

References

[1] F. Ruggiero (ed.) LHC Project Report 626, CERN, December 2002.
[2] F. Gianotti, et al., hep-ph/0204087, April 2002
[3] The ROSE Collaboration (R&D On Silicon for future Experiments), CERN-RD48 Collaboration, http://rd48.web.cern.ch/RD48/
[4] G.Lindström et al. (The RD48 Collaboration), Radiation Hard Silicon Detectors - Developments by the RD48 (ROSE) Collaboration -, Nucl. Instr. & Meth. in Phys. Res. A 466 (2001) 308-326.
[5] V. Savolainen et. al., J. Crystal. Growth, 243, 2, 2003.
[6] A. G. Bates et al., Results from the First Test Beam of a Large Microstrip Czochralski Silicon Detector Equipped with LHC Speed Electronics, LHCb-2004-052 VELO (2004).
[7] J.P.Palacios et al., Performance of a double metal n-on-n and a Czochralski silicon strip detector read out at 40 MHz, Nucl. Instr. and Meth. A 535 (2004) 428-432.
[8] J.Härkönen et al., Particle detectors made of high-resistivity Czochralski silicon, Nucl. Instr. and Meth. A 541 (2005) 202-207.
[9] P.Luukka et al., Results of proton irradiations of large area strip detectors made on high-resistivity Czochralski silicon, Nucl. Instr. and Meth. A 530 (2004) 117-121.
[10] Z. Li et. al., Radiation Hardness of High Resistivity Magnetic Czochralski Silicon Detectors After Gamma, Neutron, and Proton Radiations, IEEE Trans. on Nucl. Sci, Vol. 51, NO. 4, August 2004.
[11] T.J. Brodbeck et. al., Nucl. Instr. Meth. A 455 (2000) 645.
[12] G. Kramberger et. al, Determination of effective trapping time of electrons and holes in irradiated silicon, Nucl. Instr. and Meth. A 476 (2002) 645-651.
[13] J. Härkönen et al., Processing of Microstrip Detectors on Czochralski Grown High Resistivity Silicon Substrates, , Nucl. Instr. Meth. A 514 (2003) 173-179.
[14] M.Glaser et al., New irradiation zones at CERN-PS, Nucl. Instr. and Meth A 426 (1999) 72-77.
[15] M.Moll et al., Relation between microscopic defects and macroscopic changes in silicon detector properties after hadron irradiation, Nucl. Instr. and Meth. B 186 (2002) 100-110.
[16] M.Moll et al., Leakage current of hadron irradiated silicon detectors – material dependence, Nucl. Instr. and Meth. A (1999) 87-93.
[17] M. Moll, Radiation Damage in Silicon Particle Detectors, DESY-THESIS-1999-04 (1999).
[18] O. Kmsel, PhD thesis, Charge Collection in Irradiated Silicon Sensors in the ATLAS Pixel Detector, Dortmund University, July 2004.
[19] G. Kramberger et al., Effective trapping time of electrons and holes in different silicon materials irradiated with neutrons, protons and pions, Nucl. Instr. and Meth. A 481 (2002) 297-305
[20] E. Fretwurst et al., Survey of Recent Radiation Damage Studies at Hamburg, 3rd RD50 Collaboration Workshop, 4th November 2003.
[21] G. Kramberger, Signal development in irradiated silicon detectors, Ph.D Thesis, University of Ljubljana, 2001.
[22] V.N Abakumov et. al., Sov. Phys. Semiconductor., 12, 1 (1978)
[23] A. Hallén et al., J. Appl. Phys. 79 (1996) 3906
[24] Andreas Schramm, "Strahlenhärte von epitaktischen Siliziumdetektoren", Diploma Thesis , Institut für Experimentalphysik-Universität Hamburg, October 2003; see also RD50 Status Report 2002/2003, CERN-LHCC-2003-058 and LHCC-RD-002